Supplementary Materials: Synthesis and Complexation of Well-Defined Labeled Poly(*N*,*N*-dimethylaminoethyl methacrylate)s (PDMAEMA)

Mark Billing, Tobias Rudolph, Eric Täuscher, Rainer Beckert and Felix H. Schacher

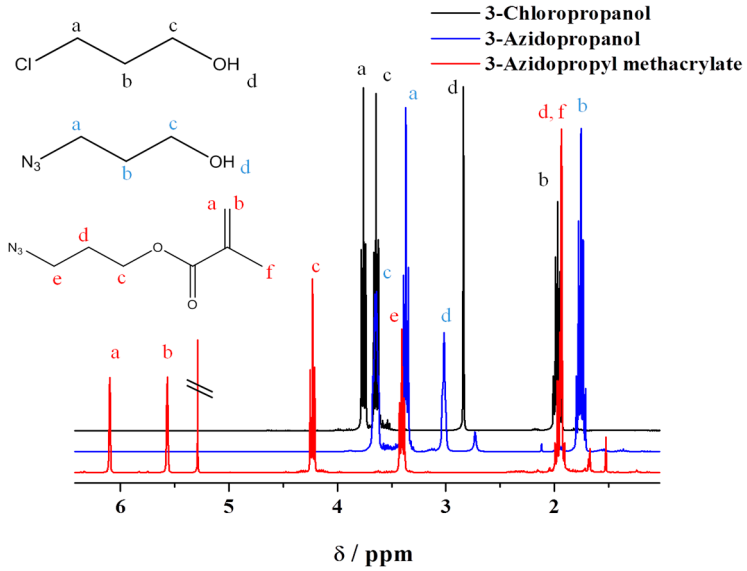

Figure S1. Comparison of ^{1}H-NMR spectra for 3-chloropropanol (black curve), 3-azidopropanol (blue curve), and 3-azidopropyl methacrylate (red curve) in $CDCl_3$.

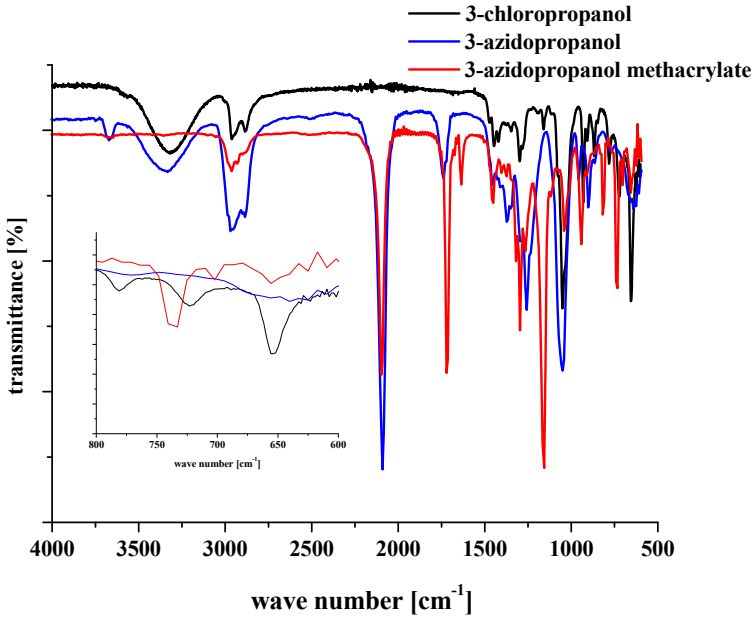

Figure S2. Comparison of FT-IR spectra of 3-chloropropanol (black line), 3-azidopropanol (blue line) and 3-azidopropyl methacrylate (red line).

Figure S2 depicts the FT-IR spectra of the intermediate stages of the monomer synthesis. The inset enlarges the finger print region, in which the disappearance of the chloride can be seen around 655 cm^{-1}.

Copolymerization of 3-Azidopropyl Methacrylate and *N,N*-Dimethylaminoethyl Methacrylate by ATRP

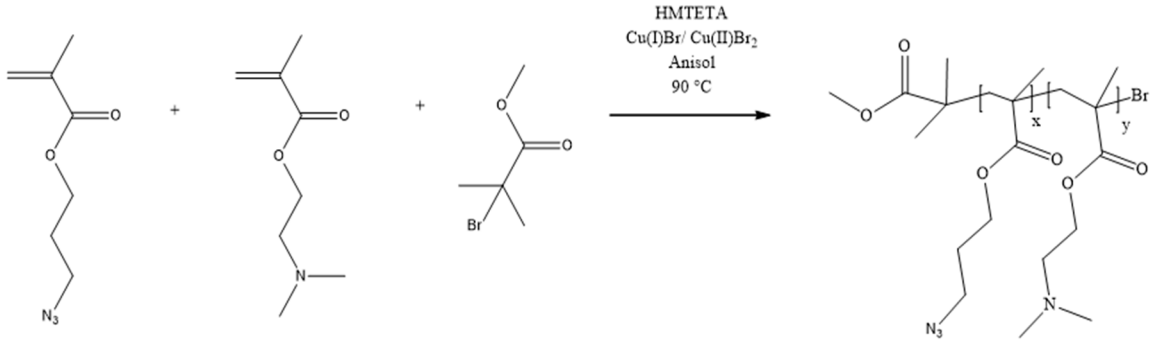

Scheme S1. Copolymerization of AzPMA and DMAEMA *via* ATRP obtaining P(AzPMA$_x$-*co*-DMAEMA$_y$).

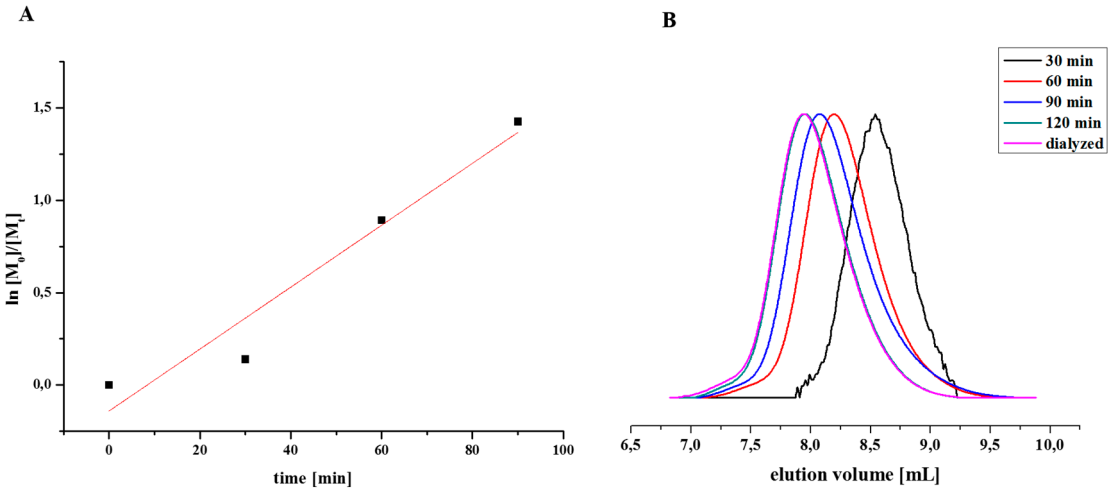

Figure S3. (**A**) Time-conversion plot for the monomer conversion during the ATRP of P(AzPMA$_{0.01}$-*co*-DMAEMA$_{0.99}$) at 90 °C in anisole; (**B**) comparison of the SEC [($CHCl_3$/TEA/*i*-PrOH. (94/2/4)): PMMA-calibration] traces obtained in the kinetic investigation of the ATRP of P(AzPMA$_{0.01}$-*co*-DMAEMA$_{0.99}$).

Table S1. Time dependent monomer conversion and molar masses of the obtained copolymers.

Time (Min)	Monomer Conversion [a] (%)	M_n [b] (g mol^{-1})	Đ [b]	M Theoretical Calculated from NMR [c]
30	13	-	-	4700
60	59	9000	1.08	18,200
90	76	11,500	1.12	23,900
120	66	12,700	1.16	20,000

[a] Determined *via* NMR; [b] Determined from SEC [($CHCl_3$/TEA/*i*-PrOH. (94/2/4)): PMMA-calibration]; [c] Determined from NMR and the initial feed ratio [M]/[I].

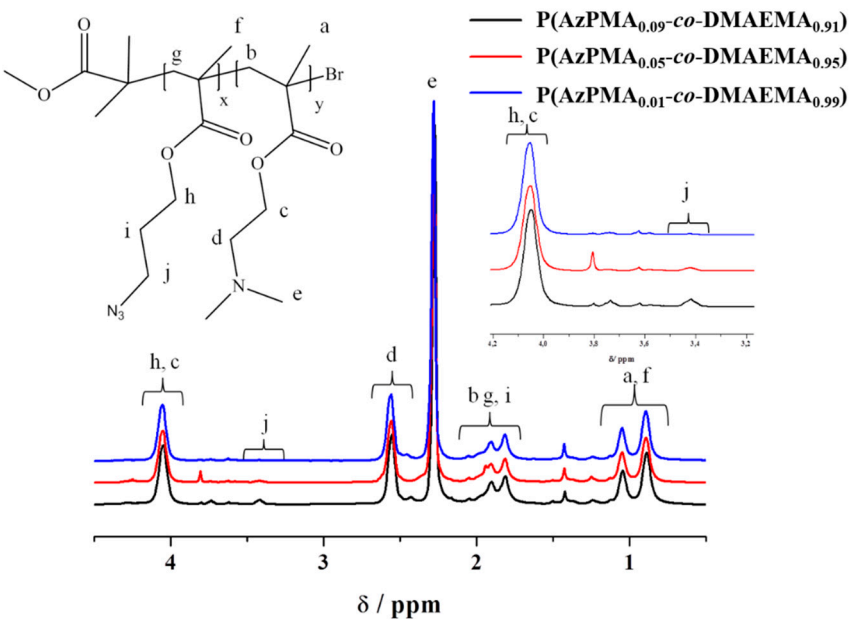

Figure S4. Comparison of ^{1}H-NMR for P(AzPMA$_x$-*co*-DMAEMA$_y$) copolymers with different composition: P(AzPMA$_{0.09}$-*co*-DMAEMA$_{0.91}$) (black curve), P(AzPMA$_{0.05}$-*co*-DMAEMA$_{0.95}$) (red curve), and P(AzPMA$_{0.01}$-*co*-DMAEMA$_{0.99}$) (blue curve) in $CDCl_3$.

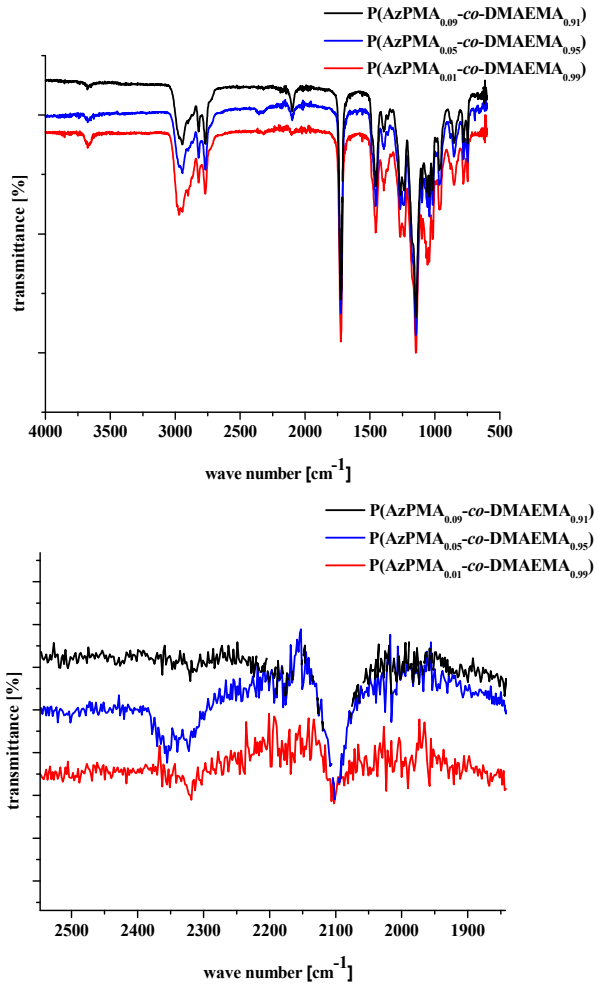

Figure S5. Comparison of the FT-IR spectra for P(AzPMA$_x$-*co*-DMAEMA$_y$) with different compositions: P(AzPMA$_{0.09}$-*co*-DMAEMA$_{0.91}$) (black curve), P(AzPMA$_{0.05}$-*co*-DMAEMA$_{0.95}$) (blue curve), and P(AzPMA$_{0.01}$-*co*-DMAEMA$_{0.99}$) (red curve).

Dye Labeled P(AzPMA*$_x$-*co*-DMAEMA$_y$) *via* Click-Chemistry

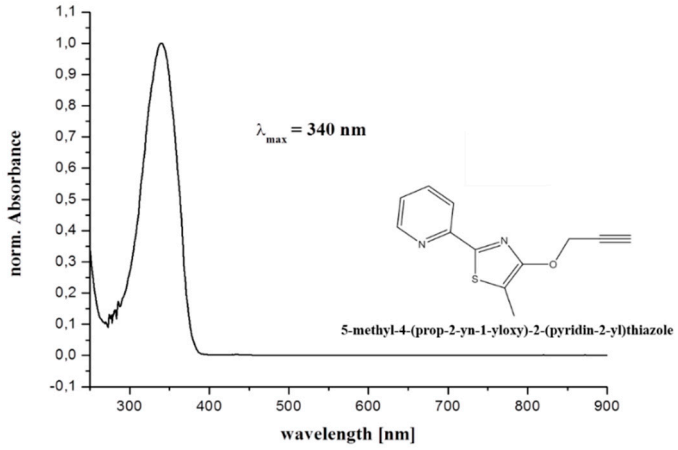

Figure S6. UV/VIS spectrum of 5-methyl-4-(prop-2-yn-1-yloxy)-2-(pyridin-2-yl)thiazole (MPPT) in THF.

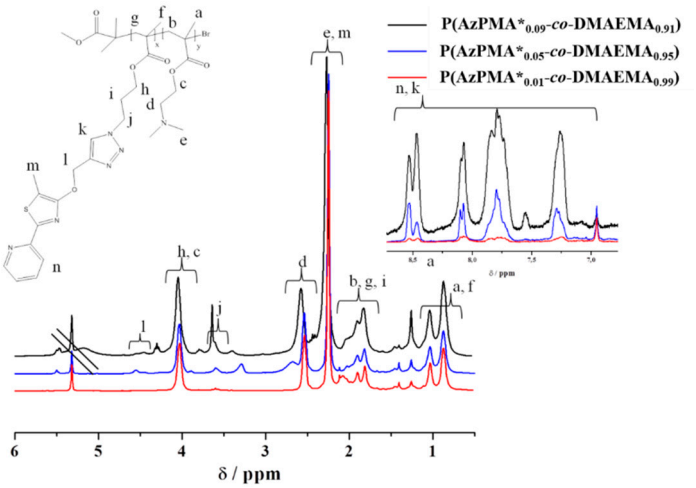

Figure S7. Comparison of ^{1}H-NMR for P(AzPMA*$_x$-*co*-DMAEMA$_y$) with different compositions: P(AzPMA*$_{0.09}$-*co*-DMAEMA$_{0.91}$) (black curve), P(AzPMA*$_{0.05}$-*co*-DMAEMA$_{0.95}$) (blue curve), and P(AzPMA*$_{0.01}$-*co*-DMAEMA$_{0.99}$) (red curve) in $CDCl_3$.

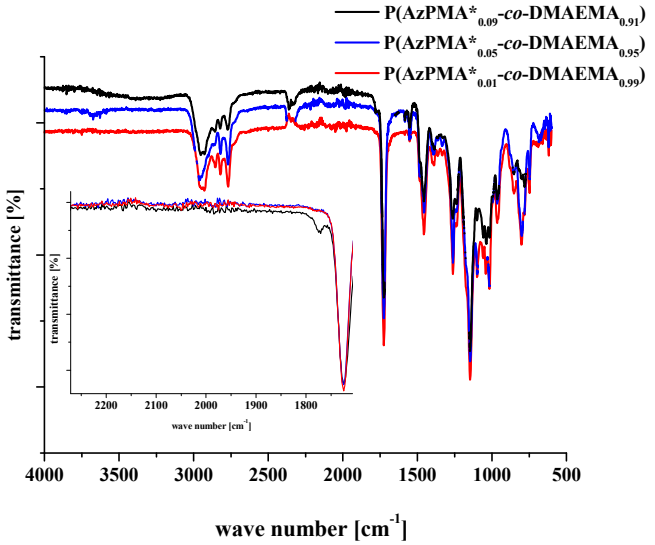

Figure S8. Comparison of the FT-IR spectra for P(AzPMA*$_x$-*co*-DMAEMA$_y$) with different compositions: P(AzPMA*$_{0.09}$-*co*-DMAEMA$_{0.91}$) (black curve), P(AzPMA*$_{0.01}$-*co*-DMAEMA$_{0.99}$) (red curve), and P(AzPMA*$_{0.05}$-*co*-DMAEMA$_{0.95}$) (blue curve).

Full conversion of the azide function was confirmed by FT-IR measurements due to the absence of the azide signal at 2100 cm^{-1}.

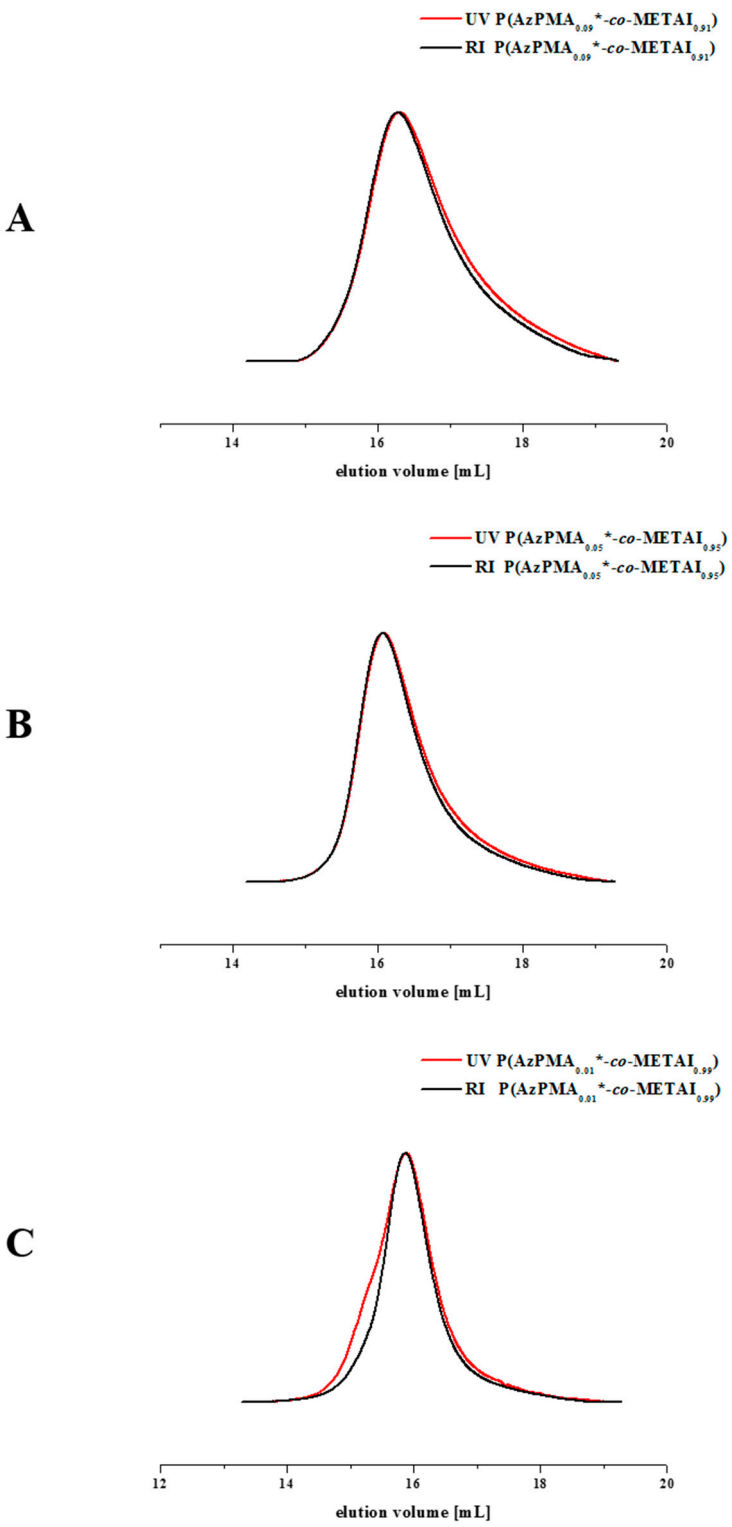

Figure S9. Comparison of SEC traces for P(AzPMA*$_x$-*co*-METAI$_y$) with different ratios of AzPMA; (**A**) P(AzPMA*$_{0.09}$-*co*-METAIA$_{0.91}$); (**B**) P(AzPMA*$_{0.05}$-*co*-METAI$_{0.95}$); (**C**) P(AzPMA*$_{0.01}$-*co*-METAI$_{0.99}$) investigated by the RI (black trace) and UV/VIS detector (red trace), Eluent: Water with 0.1% TFA and 0.1 M NaCl, detector wavelength: 360 nm.

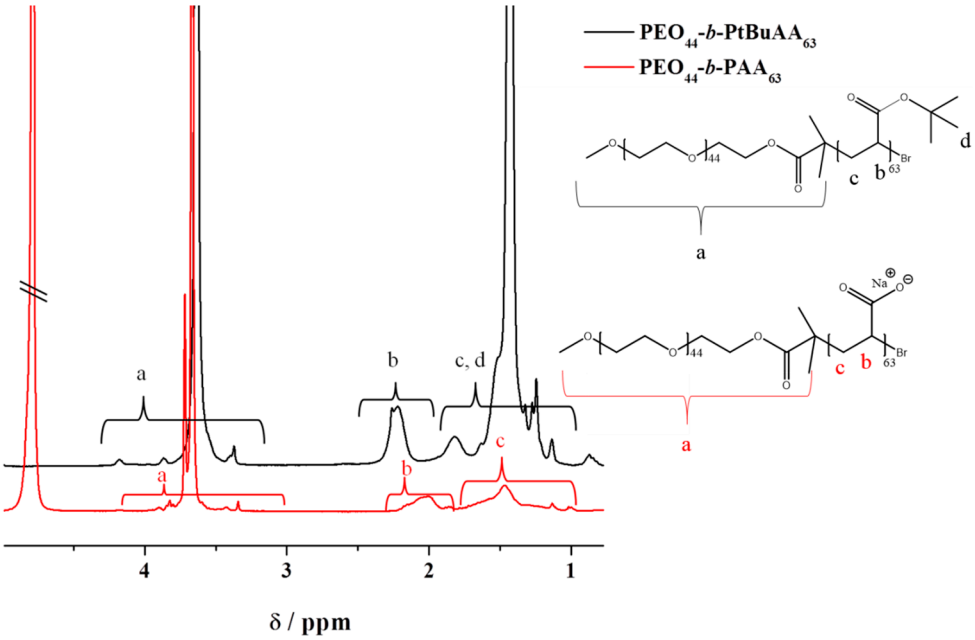

Figure S10. Comparison of ^{1}H-NMR spectra for PEO$_{118}$-*b*-P*t*BuAA$_{63}$ in $CDCl_3$ and PEO$_{118}$-*b*-PAA$_{63}$ in D_2O.

Quaternization of P(AzPMA*$_x$-*co*-DMAEMA$_y$)

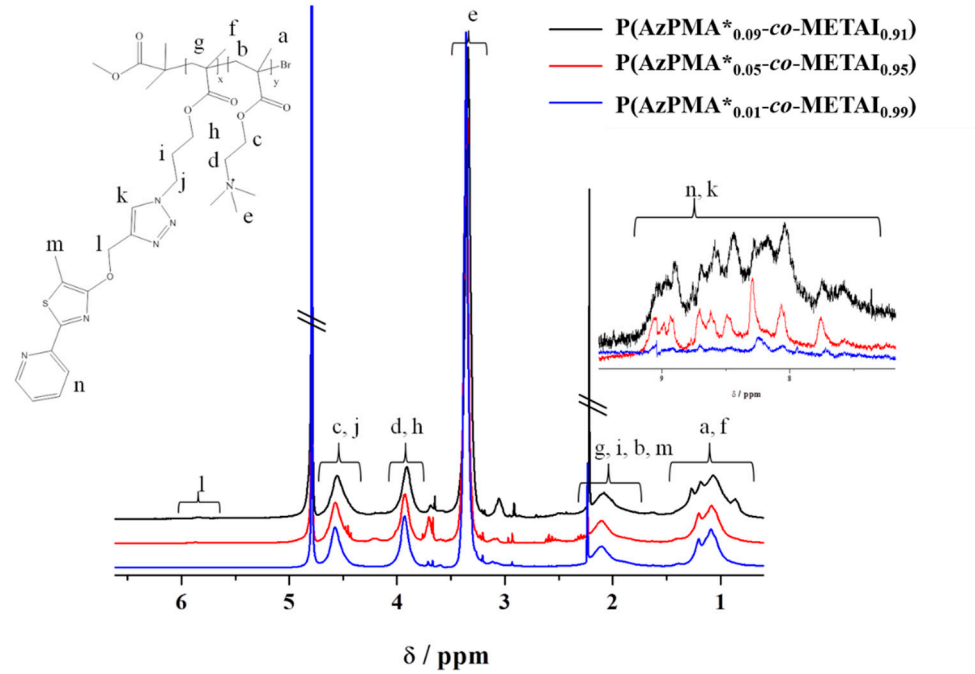

Figure S11. Comparison of ^{1}H-NMR spectra for P(AzPMA*$_x$-*co*-METAI$_y$) with different contents of AzPMA; P(AzPMA*$_{0.09}$-*co*-METAI$_{0.91}$) (black line), P(AzPMA*$_{0.05}$-*co*-METAI$_{0.95}$) (red line), P(AzPMA*$_{0.01}$-*co*-METAI$_{0.99}$) (blue line) in D_2O; the inset shows the aromatic signals of 5-methyl-4-(prop-2-yn-1-yloxy)-2-(pyridin-2-yl)thiazole (MPPT).

UV/VIS Investigations of P(AzPMA$_x$-*co*-DMAEMA$_y$), P(AzPMA*$_x$-*co*-DMAEMA$_y$) and P(AzPMA*$_x$-*co*-METAI$_y$)

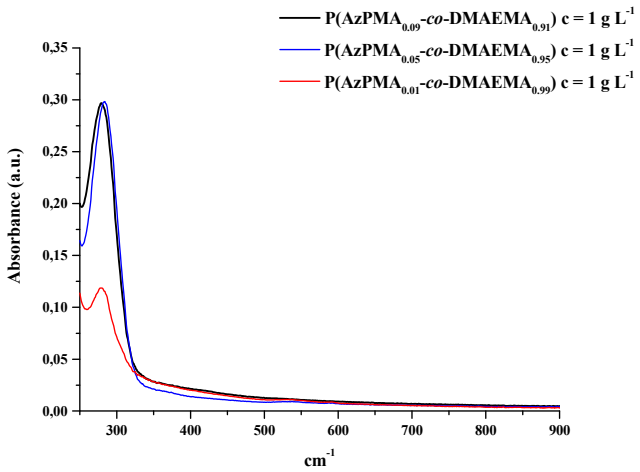

Figure S12. UV/VIS data of P(AzPMA$_{0.09}$-*co*-DMAEMA$_{0.91}$) (black curve), P(AzPMA$_{0.05}$-*co*-DMAEMA$_{0.95}$) (blue curve) and P(AzPMA$_{0.10}$-*co*-DMAEMA$_{0.99}$) (red curve) in water.

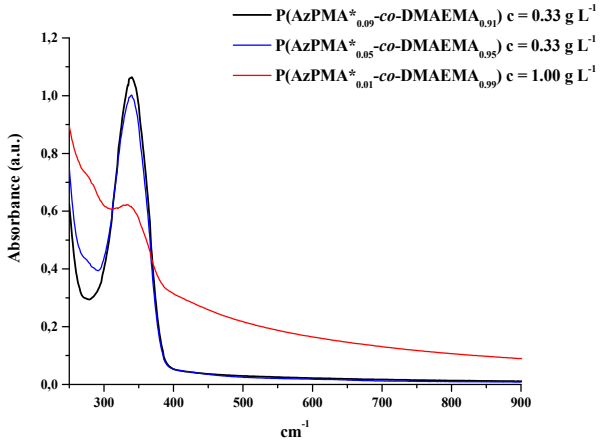

Figure S13. UV/VIS data of P(AzPMA*$_{0.09}$-*co*-DMAEMA$_{0.91}$) (black curve), P(AzPMA*$_{0.05}$-*co*-DMAEMA$_{0.95}$) (blue curve) and P(AzPMA*$_{0.01}$-*co*-DMAEMA$_{0.99}$) (red curve) in water.

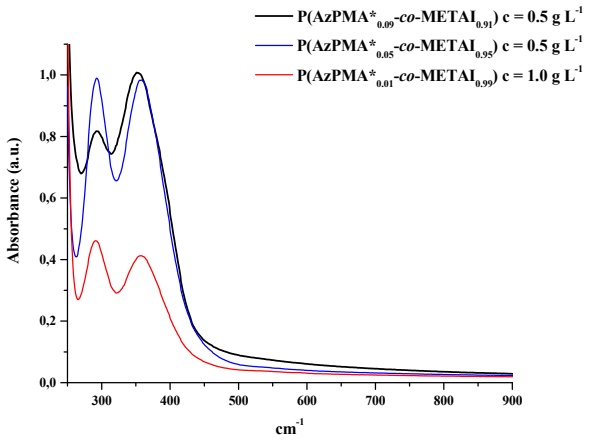

Figure S14. UV/VIS data of P(AzPMA*$_{0.09}$-*co*-METAI$_{0.91}$) (black curve), P(AzPMA*$_{0.05}$-*co*-METAI$_{0.95}$) (blue curve) and P(AzPMA*$_{0.01}$-*co*-METAI$_{0.99}$) (red curve) in water.

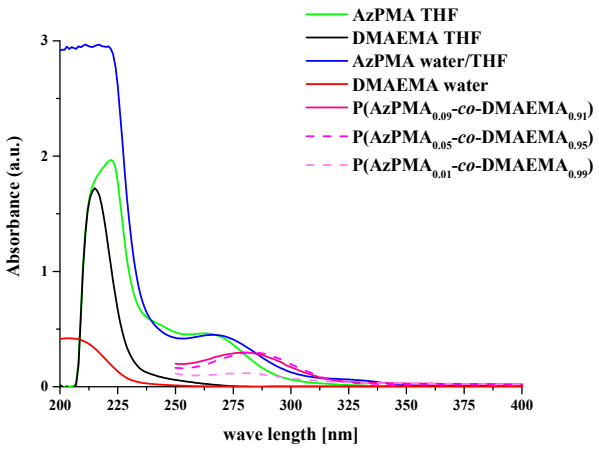

Figure S15. Comparison of UV/VIS spectra of AzPMA, DMAEMA and the resulting copolymers in water and THF.

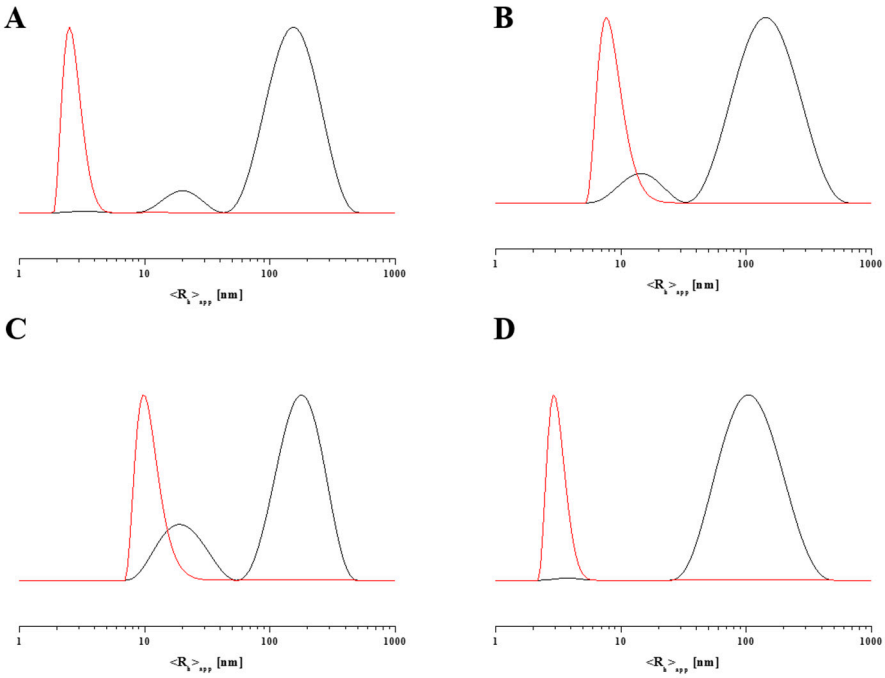

Figure S16. (**A**) DLS CONTIN plot, IPEC ($Z_{-/+}$ = 1.5) $\langle R_h \rangle_{n,app}$ = 4.8 nm (red line),) $\langle R_h \rangle_{z,app}$ = 141 nm (black line); (**B**) DLS CONTIN plot, IPEC ($Z_{-/+}$ = 1.0) $\langle R_h \rangle_{n,app}$ = 7.7 nm (red line),) $\langle R_h \rangle_{z,app}$ = 109 nm (black line);(**C**) DLS CONTIN plot, IPEC ($Z_{-/+}$ = 0.5) $\langle R_h \rangle_{n,app}$ = 10.0 nm (red line)), $\langle R_h \rangle_{z,app}$ = 113 nm (black line); (**D**) DLS CONTIN plot, IPEC ($Z_{-/+}$ = 0.25) $\langle R_h \rangle_{n,app}$ = 2.6 nm (red line),) $\langle R_h \rangle_{z,app}$ = 109 nm (black line).

Table S2. Zeta-potential measurements of P(AzPMA*$_{0.05}$-*co*-METAI$_{0.95}$), PEO$_{118}$-*b*-PAA$_{63}$ and formed IPECs ($Z_{-/+}$ = 1.5, 1.0, 0.5 and 0.25).

Sample	Voltage (mV)
P(AzPMA*$_{0.05}$-*co*-METAI$_{0.95}$)	+37
PEO$_{118}$-*b*-PAA$_{63}$	−38
$Z_{-/+}$ = 1.5	0
$Z_{-/+}$ = 1.0	0
$Z_{-/+}$ = 0.5	0
$Z_{-/+}$ = 0.25	4

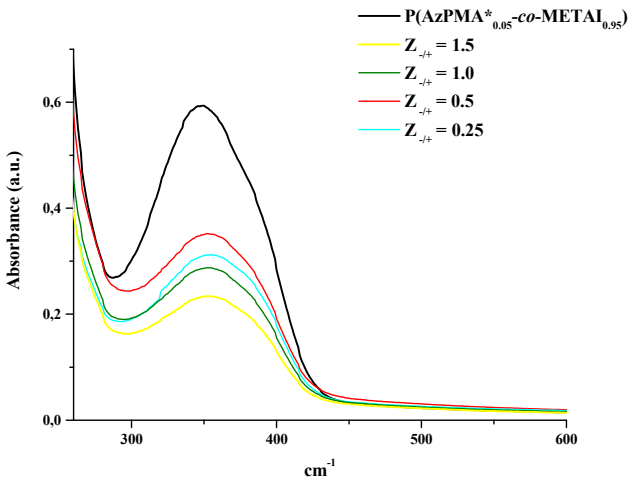

Figure S17. UV/VIS-measurement of P(AzPMA*$_{0.05}$-*co*-DMAEMA$_{0.95}$), PDMAEMA, $Z_{-/+}$ = 1.5, $Z_{-/+}$ = 1.0, $Z_{-/+}$ = 0.5, $Z_{-/+}$ = 0.25 in buffer solution at pH 10 (concentration was approximately 1 g L^{-1}).

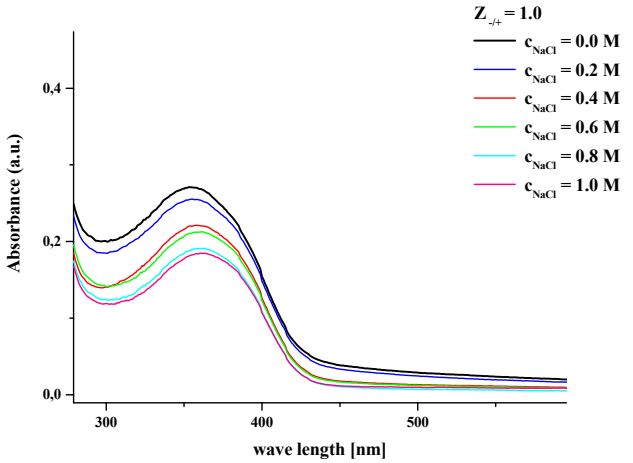

Figure S18. Variation of the ionic strength at IPEC $Z_{-/+}$ = 1.0 (1 g L^{-1}) by stepwise addition of NaCl: c_{NaCl} = 0.0 M (black curve), c_{NaCl} = 0.2 M (dark blue curve), c_{NaCl} = 0.4 M (red curve), c_{NaCl} = 0.6 M (green curve), c_{NaCl} = 0.8 M (bright blue curve), c_{NaCl} = 1.0 M (magenta curve).

Table S3. DLS data for micellar IPECs ($Z_{-/+}$ = 1.0) in buffer solution (pH 10, 1 g L^{-1}) at different ionic strength.

Conc. NaCl (M)	λ_{max} (nm)	Int.	$\langle R_h \rangle_{n,app}$ (nm)
0.0	353	0.27	8
0.2	355	0.25	3
0.4	357	0.22	2
0.6	361	0.21	2
0.8	363	0.19	2
1.0	363	0.18	2